Adv Syst Sci Appl 2025; **4**:54–69
Published online at https://ijassa.ipu.ru.

A Climate-Dependent Malaria Model with Delay in Mosquito Dynamics

Babagana Modu[1*], Savas Konur[2], Polovina Nereida[3], A. Taufiq Asyhari[4], Yonghong Peng[5]

[1] *Department of Mathematics and Statistics, Yobe State University, Damaturu, Nigeria*

[2] *Department of Computer Science, University of Bradford, UK*

[3] *Manchester Metropolitan Business School, Manchester Metropolitan University, UK*

[4] *Monash University, Indonesia*

[5] *Anglia Ruskin University, UK*

Abstract: Climate variability plays a crucial role in understanding malaria transmission dynamics, particularly through its influence on mosquito population and the parasite's developmental processes. Although temperature and rainfall have long been recognized as major climatic drivers of malaria spread, and hence most of the malaria models often overlook the combined effects of temperature-dependent aquatic-stage development and variation in the extrinsic incubation period of the parasite. This study develops a new temperature-dependent malaria transmission model that incorporates mosquito maturation delays, short- and long-term EIP routes, and an explicit aquatic-stage compartment. The model extends earlier frameworks by integrating nonlinear temperature relationships for key mosquito life-history traits and by distinguishing between short and long incubation processes through probabilistic weighting. This structure provides a more realistic representation of how climatic fluctuations regulate mosquito abundance, survival, and infectiousness. The resulting model enhances predictive accuracy in understanding malaria seasonality and transmission potential across varying environmental conditions. Numerical simulations demonstrate how temperature shifts alter the timing and intensity of outbreaks, highlighting the importance of climate-sensitive modelling for malaria surveillance and guiding adaptive vector control strategies. The proposed framework contributes to the refinement of climate-based malaria prediction tools and supports evidence-driven public health decision-making in endemic regions.

Keywords: Incubation period, Malaria transmission, Maturation delay, Mosquito dynamics, Sensitivity analysis, Temperature

1. INTRODUCTION

Understanding the influence of climate factors on malaria transmission remains a major focus of global public health research, particularly in explaining the spatial and temporal variability of malaria risk. Climatic variables such as temperature, rainfall, and humidity play distinct yet interconnected roles in understanding malaria transmission. Among these, temperature has been identified as the dominant large-scale driver of malaria transmission, directly affecting the aquatic developmental processes of mosquitoes [1], the parasite's extrinsic development period [2], mosquito survival [3], and biting rate [4]. Rainfall, in turn, generates and sustains mosquito breeding sites, increasing vector density and consequently increasing malaria

*Corresponding author: bmodu@ysu.edu.ng

transmission potential. However, excessive rainfall affect larval habitats and negatively affect mosquito survival.

Several studies have demonstrated a causal relationship between rainfall and malaria risk, highlighting the complex nonlinear relationship [5,6]. Consequently, understanding how climatic factors influence mosquito population dynamics remains crucial for predicting and mitigating vector-borne disease (VBD) outbreaks [7, 8]. The control of mosquito abundance and the reduction of human-vector contact continued to be serious challenges in malaria control strategies [9]. Hence, incorporating mosquito aquatic-stage dynamics into malaria transmission models provides a more comprehensive understanding of disease pattern and offers realistic routes for intervention design. Recent studies have increasingly investigated the effects of temperature fluctuations on malaria risk, focusing on aspects such as diurnal temperature variation, shifts in optimal temperature ranges for vector survival, and parasite development [10–12]. Other studies have explored the joint effects of temperature and rainfall on the spatio-temporal dynamics of malaria transmission [13, 14], as well as how climate variability regulates vector population and transmission potential [15, 16]. For instance, non-autonomous deterministic models have been applied to assess temperature variability and its impact on malaria transmission dynamics [17], while climate-based models incorporating periodic birth rates and vector age structures have been used to predict malaria outbreak seasons and guide public health policies [18, 19]. Furthermore, compartmental models have been deployed to investigate the role of periodic environmental changes, human mobility, and seasonal migration on malaria dynamics [20, 21]. In addition, recent modelling frameworks have focused on mosquito maturation delays and their sensitivity to temperature [22, 23], exploring nonlinear birth rates and population stability under climate variability [24, 25]. Despite these advances, limited attention has been paid to the temperature-dependent effects on the *extrinsic incubation period (EIP)*—the time required for malaria parasites to complete their development within the mosquito. This period is fundamental for determining vector infectiousness and disease persistence but is often underrepresented in climate-driven malaria models [26, 27]. Previous research primarily emphasized the human *intrinsic incubation period (IIP)* [28], which, while relevant for clinical diagnosis and outbreak detection, contributes less directly to preventive and control mechanisms in climate-sensitive malaria modelling [29]. Therefore, the EIP should be considered a more effective indicator for evaluating the influence of climate variability on malaria transmission potential. Moreover, the climate-dependent maturation delay in the aquatic stages of mosquitoes significantly determines adult female mosquito abundance. However, existing studies often model this rate as density-dependent, neglecting its spatio-temporal variability under changing environmental conditions [12, 17, 24]. The absence of this consideration limits predictive accuracy and reduces the capacity of such models to inform adaptive control strategies under different climatic scenarios.

In this study, we address these limitations by developing a new temperature-dependent malaria transmission model that explicitly incorporates mosquito dynamics and the extrinsic incubation period. Building upon the framework proposed by [21], our model introduces two categories of temperature-dependent incubation durations (short and long) for the exposed mosquito population and integrates an aquatic-stage compartment to capture the influx of adult mosquitoes through maturation. This design allows for an improved representation of temperature variability on both mosquito and parasite developmental processes. The proposed model provides deeper insights into how climatic fluctuations affect the timing and intensity of malaria transmission and offers a route for improving predictive capacity and control planning. Recent evidence highlights the growing importance of climate-based modelling for malaria surveillance and control [40–43]. By integrating EIP variability and aquatic dynamics, this study contributes to the refinement of climate-sensitive malaria models, supporting data-driven decision-making for vector control and disease prevention in endemic regions.

Copyright © 2025 ASSA.

The remainder of this paper is structured as follows. Section 2 presents the model formulation and defines the temperature-dependent parameters. Section 3 provides the theoretical analysis of the proposed mathematical model. Numerical simulations and discussions are presented in Section 4. The conclusion and recommendations for future work are presented in Section 5.

2. MODEL FORMULATION

In this section, using the schematic diagram in Fig. 2.1, we first provide a detailed description of the malaria transmission dynamics between humans and mosquitoes. Subsequently, we formulate the system of differential equations representing the proposed model and discuss its epidemiological properties, including the positivity and boundedness of solutions.

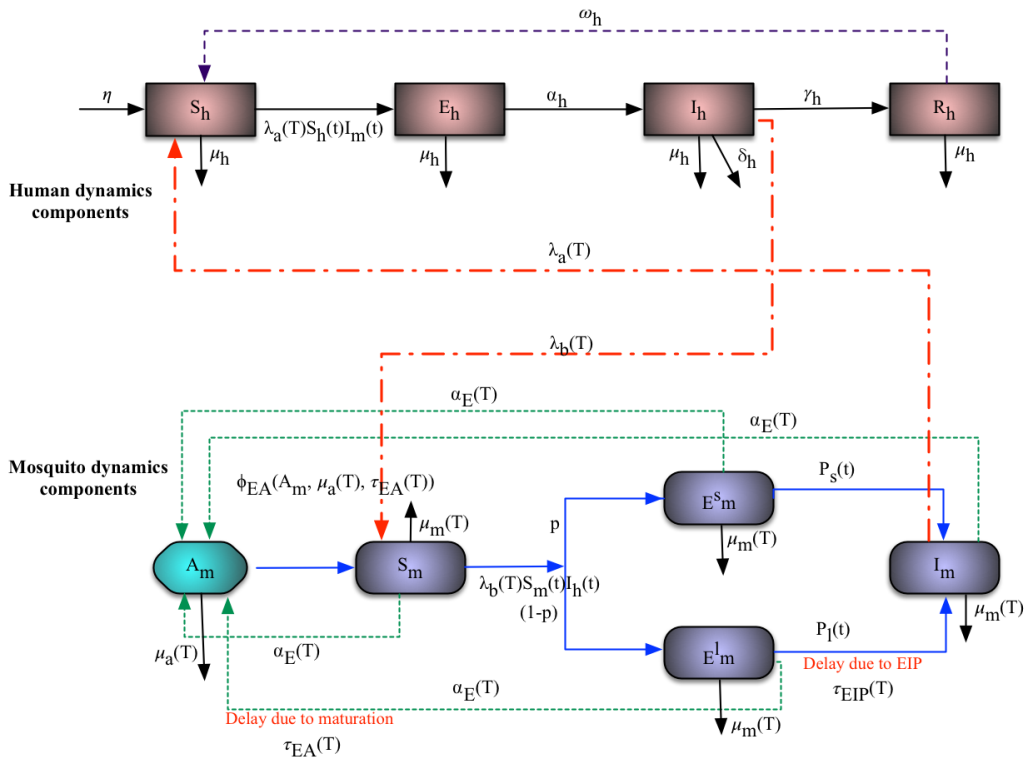

Fig. 2.1. Transition model of the malaria transmission [44].

2.1. *Model Description*

The proposed malaria transmission model in Fig. 2.1 builds upon earlier models presented in [12, 13, 21, 22], introducing key innovations. Specifically, it incorporates developmental delays linked to juvenile mosquito maturation and the extrinsic incubation period (EIP) of the parasite. These delays more accurately represent the spatiotemporal risk of malaria transmission, as both processes are strongly influenced by environmental factors such as temperature and rainfall [24].

2.1.1. Human and Mosquito Population Let $N_h(t)$ denote the total human population at time t, subdivided into four epidemiological compartments: susceptible (S_h), exposed (E_h),

Copyright © 2025 ASSA.

infectious (I_h), and recovered (R_h):

$$N_h(t) = S_h(t) + E_h(t) + I_h(t) + R_h(t) \tag{2.1}$$

Similarly, the total mosquito population $N_m(t)$ consists of immature mosquitoes (A_m) and mature mosquitoes (N_A):

$$N_m(t) = A_m(t) + N_A(t) \tag{2.2}$$

The mature mosquito population $N_A(t)$ is further subdivided into four compartments: susceptible (S_m), short-term exposed (E_m^s), long-term exposed (E_m^l), and infectious (I_m). Thus,

$$N_m(t) = A_m(t) + S_m(t) + E_m^s(t) + E_m^l(t) + I_m(t) \tag{2.3}$$

2.1.2. Aquatic Mosquito Stage Female mosquitoes require blood meals for nourishment and egg development. Eggs are typically laid in or near water bodies, progressing through larval and pupal stages before maturing into adults within 1–2 weeks, depending on environmental conditions [18]. The aquatic stage is regulated by a temperature-dependent egg deposition rate $\alpha_E(T)$ and limited by a carrying capacity K_c, such that:

$$\alpha_E(T)\left[1 - \frac{A_m(t)}{K_c}\right](S_m(t) + E_m^s(t) + E_m^l(t) + I_m(t)).$$

The maturation process is delayed by $\tau_1(T)$, representing the mean development time from egg to adult, with $\mu_a(T)$ denoting the immature-stage mortality rate. The survival probability of aquatic mosquitoes is $e^{-\mu_a(T)\tau_1(T)}$, and the maturation into adults is represented as:

$$p_{EA}(\hat{T})A_m(t - \tau_1(T))e^{-\mu_a(T)\tau_1(T)}e^{-A_m(t-\tau_1(T))}.$$

Mosquitoes become infected at a temperature-dependent transmission rate $\lambda_b(T)$ after biting an infectious human. Following blood ingestion, they experience a resting phase for egg development, during which they may die at rate $\mu_m(T)$. Rainfall affects mosquito abundance by creating or destroying breeding habitats—while moderate rainfall enhances breeding, excessive rainfall can flush larvae from breeding sites.

2.1.3. Extrinsic Incubation Period Adult mosquitoes that ingest *Plasmodium* gametocytes from infected humans become exposed but not immediately infectious. The parasite undergoes an Extrinsic Incubation Period (EIP)—typically 10–14 days [8]—before migrating to the mosquito's salivary glands, after which the mosquito becomes infectious. The duration of this period depends heavily on temperature; lower temperatures extend the EIP, whereas higher temperatures shorten it. Consequently, EIP variation is a critical determinant of malaria transmission potential.

To account for environmental heterogeneity, we introduce two exposed mosquito states: short-term (E_m^s) and long-term (E_m^l) EIPs. While a similar approach has been applied to incubation in human [21], our formulation distinctively models mosquito incubation dynamics as temperature-dependent.

2.1.4. Exposed Mosquitoes Dynamics Exposed mosquitoes remain in the latent stage until they either complete their extrinsic incubation period (EIP) or die. Their population dynamics are represented by:

$$E_m(t) = \int_0^\infty \beta_{hm}\Phi(S_m, I_h)e^{-\mu_m u}P(u)\,du, \tag{2.4}$$

where $\Phi(S_m, I_h) = S_m(t-u)I_h(t-u)$, and $P(u)$ denotes the probability that an exposed mosquito remains in the latent stage at time u. The function $P(u)$ satisfies the following

Copyright © 2025 ASSA.

properties: (i) $P : [0, \infty) \to [0, 1]$ is non-increasing, piecewise continuous, with $P(0^+) = 1$ and $\lim_{u\to\infty} P(u) = 0$; (ii) The integrand of $P(u)$ is strictly positive for $u \in (0, 1)$. To distinguish between short-term and long-term EIPs, we introduce $p \in (0, 1)$ as the probability that a mosquito experiences a short-term incubation period. Thus,

$$P(u) = pP_s(u) + (1 - p)P_l(u),$$

where $P_s(u)$ and $P_l(u)$ represent the short- and long-term EIP components, respectively. The short-term EIP follows an exponential distribution with rate $\theta(T)$:

$$P_s(u; \theta(T)) = \theta(T)e^{-\theta(T)u}, \quad u > 0, \tag{2.5}$$

while the long-term EIP is modelled as a step function of duration τ:

$$P_l(u) = \begin{cases} 1, & 0 \le u \le \tau, \\ 0, & u > \tau. \end{cases} \tag{2.6}$$

Substituting (2.5) and (2.6) into (2.4) yields:

$$\begin{aligned} E_m^s(t) &= \int_0^\infty p\lambda_b(T)\Phi(S_m, I_h)e^{-\mu_m u}P_s(u)\, du, \\ E_m^l(t) &= \int_0^\tau (1 - p)\lambda_b(T)\Phi(S_m, I_h)e^{-\mu_m u}P_l(u)\, du. \end{aligned} \tag{2.7}$$

Differentiating (2.7) gives the dynamic equations:

$$\begin{aligned} \dot{E}_m^s(t) &= p\Gamma_2 - \Gamma_1 E_m^s(t), \\ \dot{E}_m^l(t) &= (1 - p)\Gamma_2 - \mu_m(T)E_m^l(t), \end{aligned} \tag{2.8}$$

where $\Gamma_1 = \mu_m(T) + \theta_m(T)$ and $\Gamma_2 = \lambda_b(T)S_m(t)I_h(t) - \lambda_b(T)\psi(\tau_2, \mu_m, T)$.This formulation captures both short- and long-term extrinsic incubation routes, enabling a more realistic representation of temperature-dependent mosquito infection dynamics.

The malaria transmission dynamics in Fig. 2.1 are governed by the following system of nonlinear differential equations:

$$\begin{cases} \dot{S}_h(t) = \eta - \Gamma_6 - \mu_h S_h(t) + \omega_h R_h(t), \\ \dot{E}_h(t) = \Gamma_6 - (\alpha_h + \mu_h)E_h(t), \\ \dot{I}_h(t) = \alpha_h E_h(t) - (\mu_h + \delta_h + \gamma_h)I_h(t), \\ \dot{R}_h(t) = \gamma_h I_h(t) - (\mu_h + \omega_h)R_h(t), \\ \dot{A}_m(t) = \Gamma_4 - \mu_a(T)A_m(t) - \Gamma_5, \\ \dot{S}_m(t) = \Gamma_5 - \Gamma_2 - \mu_m(T)S_m(t), \\ \dot{E}_m^s(t) = p\Gamma_2 - \Gamma_1 E_m^s(t), \\ \dot{E}_m^l(t) = (1 - p)\Gamma_2 - \mu_m(T)E_m^l(t), \\ \dot{I}_m(t) = \theta_m(T)E_m^s(t) + (1 - p)\Gamma_3 - \Gamma_7, \end{cases} \tag{2.9}$$

The parameters, $\Gamma_1, \cdots, \Gamma_7$ are rescaled from the model (2.9) to simplify the system and reduce the complexity of its underlying dynamics.

$$\Gamma_3 = \lambda_b(T)\psi(\tau_2, \mu_m, T), \quad \Gamma_4 = \alpha_E(T)\left[1 - \frac{A_m(t)}{K_c}\right]N_A(t), \quad \Gamma_5 = \phi_{EA}(T)\varphi(\tau_1, \mu_a, \hat{T}),$$

Copyright © 2025 ASSA.

$$\Gamma_6 = \lambda_a(T)S_h(t)I_m(t), \quad \Gamma_7 = \mu_m(T)I_m(t).$$

The initial conditions of the system (2.9) are given by:

$$S_h(0) > 0, \quad E_h(0) \geq 0, \quad I_h(0) \geq 0, \quad R_h(0) \geq 0, \quad A_m(0) > 0,$$

$$S_m(\theta) = \phi_{sm}(t) > 0, \quad E_m^s(0) \geq 0, \quad E_m^l(0) \geq 0, \quad I_m(\theta) = \phi_{im}(t) > 0,$$

where $\phi_{sm}(\theta)$ and $\phi_{im}(\theta)$ are continuous functions for $\theta \in [-\tau, 0]$. For simplicity, some differential equations in the system (2.9) are rescaled by redefining $\varphi(\tau_1, \mu_a, \hat{T})$ and $\psi(\tau_1, \mu_m, T)$ as:

$$\begin{aligned} \varphi(\tau_1, \mu_a, \hat{T}) &= A_m(t - \tau_1(\hat{T}))e^{-\mu_a(T)\tau_1(\hat{T})}e^{-A_m(t-\tau_1(\hat{T}))}, \\ \psi(\tau_1, \mu_m, T) &= S_m(t - \tau_1(T))I_h(t - \tau_1(T))e^{-\mu_m(T)\tau_1(T)}. \end{aligned} \tag{2.10}$$

The egg-to-adult survival probability, $\phi_{EA}(T)$, is given by:

$$\phi_{EA}(T) = -0.00924\hat{T}^2 + 0.453\hat{T} - 4.77,$$

as reported in [10]. The transmission forces are represented by:

$$\lambda_a(T) = bc_m(T) = abm, \qquad \lambda_b(T) = ac_m(T).$$

The definitions and numerical values of all state variables and parameters are presented in Tables 2.1 – 3.3. In the system (2.9) and equation (2.10), all temperature-dependent parameters are assumed to be continuous, bounded, positive, and ω-periodic. Following [13], we define $T = T(t)$ and $\hat{T} = T(t) + \delta_T$ to represent the air and water temperatures at time t, respectively.

2.1.5. Temperature-Dependent Parameters Several key parameters in the model are temperature-dependent, notably the adult mosquito biting rate $c_m(T)$, mortality rate $\mu_m(T)$, and egg deposition rate $\alpha_E(T)$. Their temperature relationships are expressed as quadratic functions [10]:

$$\begin{aligned} c_m(T) &= -0.00014T^2 + 0.027T - 0.322, \\ \mu_m(T) &= -\ln(-0.000828T^2 + 0.0367T + 0.522), \\ \alpha_E(T) &= -0.153T^2 + 8.61T - 97.7. \end{aligned} \tag{2.11}$$

Rainfall also influences mosquito development, especially during the aquatic stages. Excessive rainfall can reduce survival by washing away larvae from breeding sites. The temperature-dependent mortality rate of immature mosquitoes, $\mu_a(T)$, is modelled as [28]:

$$\mu_a(T) = \left[8.560 + 20.654\left(1 + \left(\frac{T}{19.759}\right)^{6.827}\right)^{-1}\right]^{-1}. \tag{2.12}$$

Equations (2.11) and (2.12) illustrate the nonlinear and interdependent effects of temperature and rainfall on mosquito dynamics, as depicted in Fig. 2.2.

Copyright © 2025 ASSA.

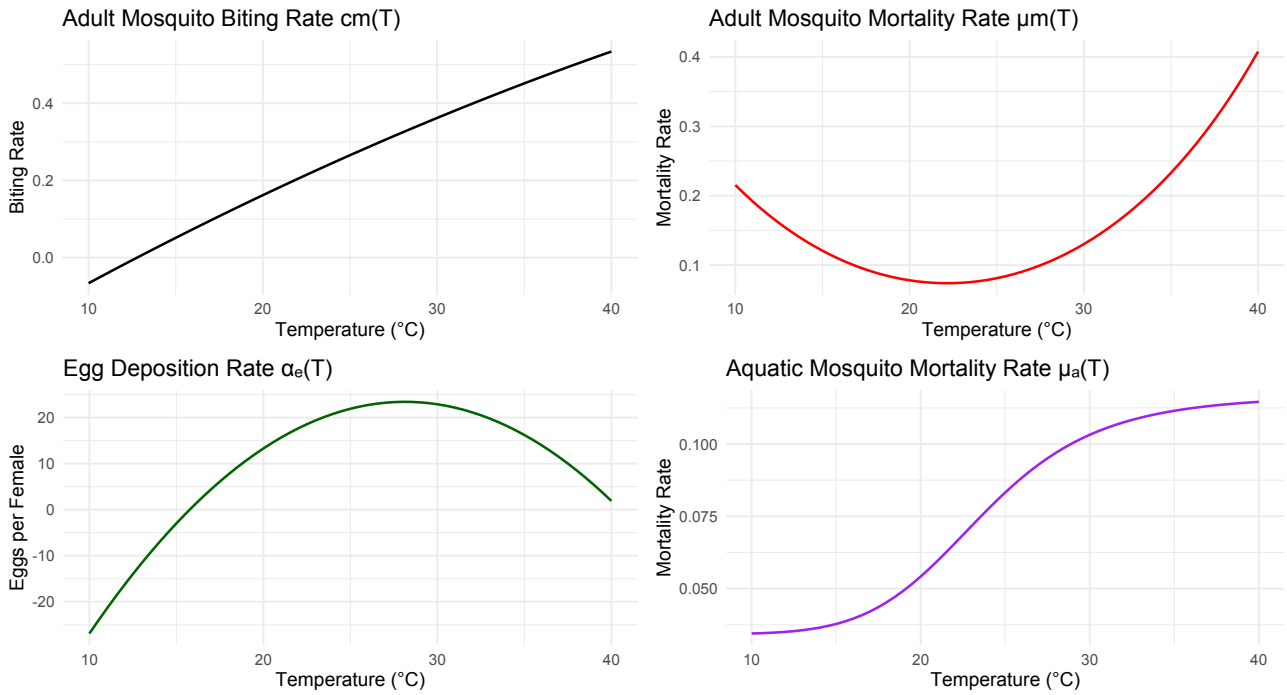

Fig. 2.2. Nonlinear effects of temperature and rainfall on mosquito dynamics.

Table 2.1. Definition of states variable.

Symbol	Definition
$S_h(t)$	Number of susceptible humans at time t.
$E_h(t)$	Number of exposed humans undergoing the latent period at time t.
$I_h(t)$	Number of infectious humans at time t.
$R_h(t)$	Number of recovered (or removed) humans at time t.
$A_m(t)$	Population of aquatic-stage mosquitoes at time t.
$S_m(t)$	Population of susceptible adult female mosquitoes at time t.
$E_m^s(t)$	Population of exposed adult female mosquitoes undergoing short-term latency at time t.
$E_m^l(t)$	Population of exposed adult female mosquitoes undergoing long-term latency at time t.
$I_m(t)$	Population of infectious adult female mosquitoes at time t.

3. MATHEMATICAL ANALYSIS

In this section, the theoretical analysis of system (2.9) and explores its fundamental analytical properties within a biologically meaningful context.

3.1. Total Human Population

From system (2.9), the total human population is defined as

$$N_h(t) = S_h(t) + E_h(t) + I_h(t) + R_h(t).$$

The rate of change of $N_h(t)$ is obtained as follows:

$$\begin{aligned} N_h'(t) &= \eta - \mu_h S_h - \mu_h E_h - \mu_h I_h - \mu_h R_h - \delta_h I_h \\ &= \eta - \mu_h N_h - \delta_h I_h \\ &\leq \eta - \mu_h N_h. \end{aligned} \tag{3.13}$$

Copyright © 2025 ASSA.

Table 2.2. Definition of parameters.

Symbol	Definition
η	Recruitment rate of humans into the susceptible class.
ω_h	Rate of loss of immunity among recovered humans.
μ_h	Natural death rate of humans.
μ_m	Natural death rate of adult female mosquitoes.
μ_a	Natural death rate of aquatic-stage mosquitoes.
α_E	Egg deposition rate per adult female mosquito.
p	Probability that an exposed mosquito undergoes short-term latency.
α_h	Rate at which exposed humans progress to the infectious stage.
γ_h	Recovery rate of infectious humans.
θ_m	Rate at which exposed mosquitoes become infectious.
τ_2	Incubation delay period of malaria parasites in humans.
a	Probability of malaria transmission from an infectious mosquito to a susceptible human.
b	Probability of malaria transmission from an infectious human to a susceptible mosquito.
c_m	Per capita biting rate of mosquitoes on humans.
m	Ratio of mosquito population to human population.
ϕ_{EA}	Recruitment rate of adult female mosquitoes from aquatic stages.
K_c	Carrying capacity of the aquatic mosquito population.
τ_1	Maturation delay period of immature mosquitoes.
δ_h	Malaria-induced death rate of infectious humans.
λ_a	Force of infection for susceptible humans.
λ_b	Force of infection for susceptible mosquitoes.

Equation (3.13) shows that the total human population is ultimately bounded by the balance between recruitment (η) and natural mortality ($\mu_h N_h$), with disease-induced deaths $\delta_h I_h$ further reducing population size.

3.2. Total Mosquito Population

Similarly, the total mosquito population is given by

$$N_m(t) = A_m(t) + S_m(t) + E_m^s(t) + E_m^l(t) + I_m(t).$$

Differentiating with respect to time yields:

$$\begin{aligned} N_m'(t) &= \Gamma_4 N_A(t) - \mu_a(t) A_m(t) - \mu_m(t)\big[N_m(t) - A_m(t)\big] \\ &= \Gamma_4 N_A(t) - \mu(t) N_m(t), \end{aligned} \tag{3.14}$$

where $\mu(t) = \min(\mu_a(t), \mu_m(t))$ denotes the effective mortality rate of mosquitoes [12].

3.3. Boundedness and Positivity of Solutions

Since the system (2.9) is non-autonomous, malaria transmission is analyzed under a periodic environmental framework. Following [14], it is assumed that the mosquito population stabilizes at a periodic equilibrium. Hence, there exists a positive constant h_0 such that:

$$N_m'(t) = \Gamma_4 N_A(t) - \mu(t) L < 0, \quad \forall L \geq h_0. \tag{3.15}$$

Given non-negative initial conditions, the system (2.9) ensures $N_h(t) > 0$ for all $t \geq 0$. Consequently, it admits a unique, non-negative solution in $C([0,\infty), \mathbb{R}_+^9)$, with all trajectories ultimately bounded and uniformly stable.

3.4. Existence and Positivity of Solutions

Following the formulation in [16], the system (2.9) can be expressed in vector form as:

$$\dot{X}(t) = B(X)X + H, \tag{3.16}$$

Copyright © 2025 ASSA.

where

$$X = (S_h, E_h, I_h, R_h, A_m, S_m, E_m^s, E_m^l, I_m)^T, \quad H = (\eta, 0, 0, 0, 0, 0, 0, 0, 0)^T.$$

The matrix $B(X)$ is a *Metzler matrix*, meaning that all its off-diagonal entries are non-negative. Consequently, the system is *positively invariant* in $\mathbb{R}^9_+$; that is, any trajectory that begins in the positive orthant remains there for all $t \geq 0$. This property guarantees the biological feasibility of the model, ensuring that all population compartments remain non-negative over time.

By applying the *comparison principle* [29], the total human and mosquito populations satisfy:

$$\limsup_{t\to\infty} N_h(t) \leq \frac{\eta}{\mu_h}, \quad \limsup_{t\to\infty} [N_m(t) - N_m^*(t)] \leq 0,$$

where $N_m^*(t)$ denotes the unique ω-periodic positive solution of (3.14), given by:

$$N_m^*(t) = e^{-\int_0^t \mu_m(s)\,ds} \left\{ \Gamma_9 + \Gamma_{10} \right\}, \tag{3.17}$$

with

$$\Gamma_9 = \int_0^t \alpha_E(s) \left(1 - \frac{A_m(s)}{K_c}\right) N_A(s) e^{\int_0^s \mu_m(\omega)\,d\omega}\,ds, \tag{3.18}$$

and

$$\Gamma_{10} = \frac{\int_0^\tau \alpha_E(s) \left(1 - \frac{A_m(s)}{K_c}\right) N_A(s) e^{\int_0^s \mu_m(\omega)\,d\omega}\,ds}{e^{\int_0^\tau \mu_m(s)\,ds} - 1}. \tag{3.19}$$

Therefore, all solutions of system (2.9) are *uniformly bounded* and remain positive for all $t \geq 0$ [14]. This establishes the existence, uniqueness, and biological consistency of the model solutions.

Table 3.3. Baseline parameter values and range.

Symbol	Baseline	Range	Reference
η	4×10^{-5}/day	$(3.91 - 5) \times 10^{-5}$/day	[21]
ω_h	1.7×10^{-5}/day	$5.5 \times 10^{-5} - 1.1 \times 10^{-2}$/day	[13]
μ_h	4×10^{-5}/day	$(3.42 - 3.91) \times 10^{-5}$/day	[13]
μ_m	5×10^{-2}/day	$(4.76 - 7.14) \times 10^{-2}$/day	[13, 36]
μ_a	1.04×10^{-1}/day	$1 \times 10^{-3} - 2 \times 10^{-1}$/day	[12–14]
α_E	1.84/day	$1 - 500$/day	[12–14]
p	0.25	-	[21]
α_h	5×10^{-3}	$(2 - 7) \times 10^{-3}$	[12]
γ_h	2.3×10^{-3}/day	$1.4 \times 10^{-3} - 1.7 \times 10^{-2}$/day	[13]
θ_m	9.1×10^{-2}/day	$2.9 \times 10^{-2} - 3.3 \times 10^{-1}$/day	[13]
τ_2	10	$10 - 14$/days	[37]
a	2.4×10^{-1}/day	$7.2 \times 10^{-2} - 6.4 \times 10^{-1}$/day	[12, 13, 36, 38]
b	2.2×10^{-2}/day	$2.7 \times 10{-}3 - 6.4 \times 10^{-1}$/day	[12, 13, 38]
c_m	0.29/day	$0.10 - 1.0$/day	[12, 13, 36, 38]
m	2	-	[21]
ϕ_{EA}	0.343/day	$0.333 - 1.0$	[12]
K_c	4×10^4	$50 - 3.3 \times 10^6$	[12, 13]
τ_1	12	$10 - 37$days	[10, 12]
δ_h	3.454×10^{-4}	$0 - 4.1 \times 10^{-4}$/day	[13]

Copyright © 2025 ASSA.

3.5. Basic Reproduction Number

The basic reproduction number, denoted by R_0, represents the expected number of secondary infections produced by one infected individual introduced into a wholly susceptible population. Following the next-generation matrix approach [13], we express R_0 as the spectral radius (dominant eigenvalue) of the matrix $\mathcal{F}\mathcal{V}^{-1}$, i.e.,

$$R_0 = \rho(\mathcal{F}\mathcal{V}^{-1}). \tag{3.20}$$

The analytical approximation of R_0 for the malaria transmission model is given by:

$$R_0 = \sqrt{\frac{\beta_{mh}\,\beta_{hm}\,S_h^0\,S_m^0\,\alpha_h\,\theta_m(T)}{N_h^2\,(\alpha_h+\mu_h)\,(\mu_h+\delta_h+\gamma_h)\,\mu_m(T)^2}}, \tag{3.21}$$

where β_{mh} and β_{hm} denote the transmission probabilities per bite from mosquito to human and human to mosquito, respectively, while $\theta_m(T)$ and $\mu_m(T)$ represent the temperature-dependent mosquito progression and mortality rates. The adult mosquito mortality rate is temperature-dependent and given by [10]:

$$\mu_m(T) = -\ln\left(-0.000828T^2 + 0.0367T + 0.522\right), \tag{3.22}$$

valid for the temperature range $16^\circ\mathrm{C} \le T \le 34^\circ\mathrm{C}$.

4. NUMERICAL ANALYSIS

In this section, we present a comprehensive numerical evaluation of the temperature-dependent basic reproduction number, followed by simulations of the state variables and sensitivity analysis.

4.1. Evaluation of R_0

Using the baseline parameter values presented in Table 3.3 and setting $\beta_{mh} = c_m b$, $\beta_{hm} = c_m a$, and $N_h = \eta/\mu_h$, the baseline R_0 at $T = 25^\circ\mathrm{C}$ is numerically estimated as:

$$R_0(25^\circ\mathrm{C}) \approx 7.34.$$

This indicates that, under the given assumptions, one infectious individual can generate approximately seven new secondary infections in a fully susceptible population at 25°C, highlighting high transmission potential under optimal conditions.

Fig. 4.3 shows the variation of R_0 with temperature for three different mosquito incubation rates $\theta_m = 0.071,\ 0.091$, and 0.1 day^{-1}. The results demonstrate that R_0 increases with temperature up to approximately 22–23°C, beyond which it declines due to elevated mosquito mortality. The maximum transmission potential therefore occurs at moderate temperatures.The horizontal dashed line indicates the epidemic threshold $R_0 = 1$.

Table 4.4. Basic reproduction number R_0 at different temperature levels.

Temperature (°C)	R_0
18	0.72
22	1.15
25	1.45
28	1.63
32	0.98

Copyright © 2025 ASSA.

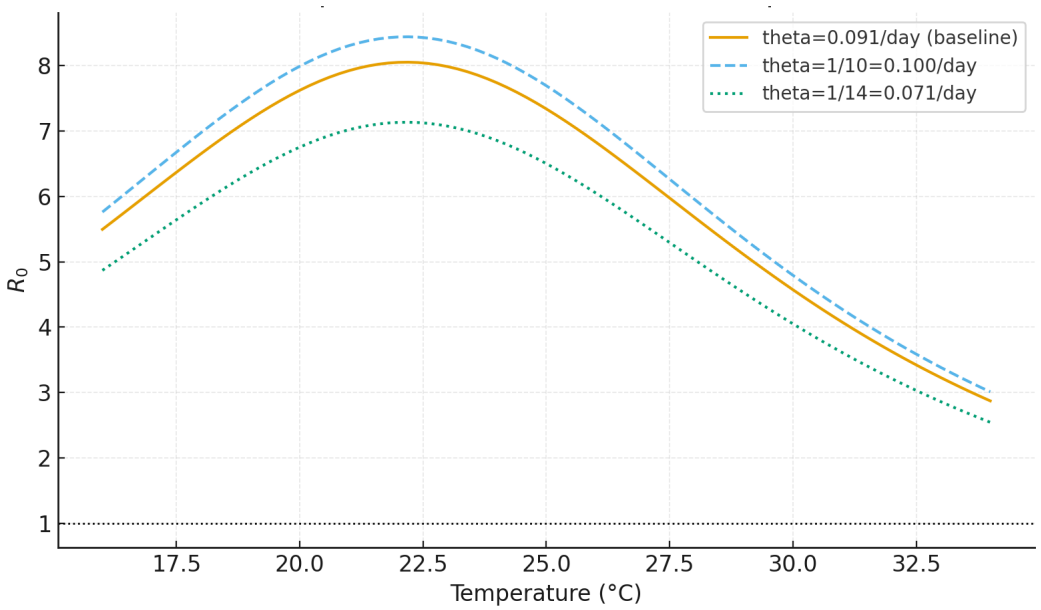

Fig. 4.3. Variation of the R_0 and mosquito incubation rates θ_m.

The results presented in Table 4.4 show that the basic reproduction number, R_0, varies substantially with temperature, revealing a distinct optimal range for malaria transmission. At lower temperatures, such as $18°$C, R_0 remains below the epidemic threshold ($R_0 = 0.72$), indicating that transmission cannot be sustained. As temperature increases, transmission potential improves, with R_0 exceeding 1 at $22°$C and continuing to rise, reaching its peak value of 1.63 at $28°$C, where mosquito survival, biting activity, and parasite development are most favorable. However, at $32°$C, R_0 declines to 0.98, suggesting that excessively high temperatures begin to impair vector and parasite dynamics. Overall, the findings indicate that malaria transmission is most efficient within the moderate temperature range of 22–$28°$C, with optimal conditions occurring near $28°$C.

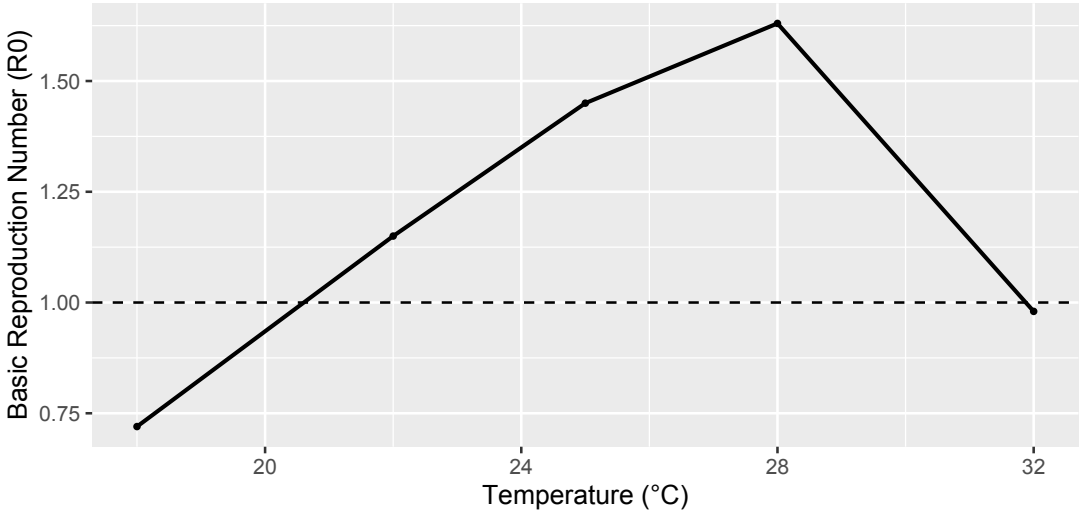

Fig. 4.4. Relationship between R_0 and temperature.

Fig, 4.5 shows that shorter mosquito incubation delays lead to a rapid decline in susceptible humans due to faster transmission, whereas longer delays result in weaker

Copyright © 2025 ASSA.

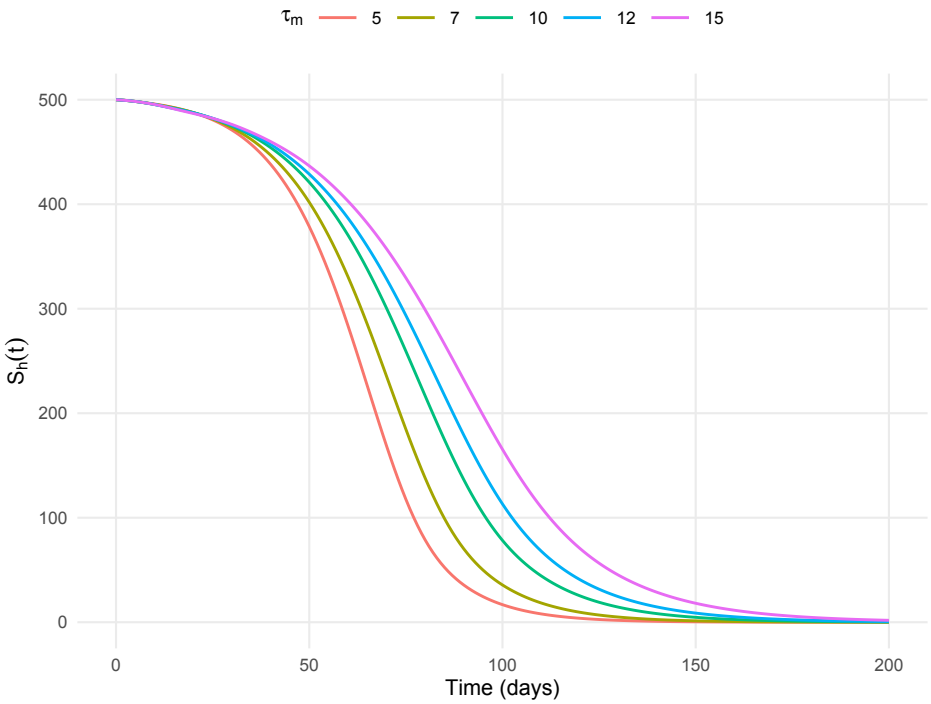

Fig. 4.5. Human susceptibility at different τ_m = 5, 7, 10, 12, 15.

transmission and a larger remaining susceptible population. The shorter incubation periods (often at warmer temperatures) enhance malaria spread, while longer delays (associated with cooler conditions) limit transmission.

4.2. Sensitivity Analysis

To assess the relative importance of the key parameters on the basic reproduction number R_0, a local sensitivity analysis was performed. The normalized sensitivity index for each parameter x_i is defined as [45]:

$$S_{x_i} = \frac{\partial R_0}{\partial x_i} \cdot \frac{x_i}{R_0}.$$

The indices quantifies the proportional change in R_0 resulting from a 1% change in each parameter. Table 4.5 lists the calculated elasticity values. Figure 4.6 illustrates these results

Table 4.5. Sensitivity indices of R_0 with respect to model parameters.

Parameter	**Elasticity Value**
$b\ (\beta_{hm})$	22.7276
θ_m	5.4946
$a\ (\beta_{mh})$	2.0834
α_h	0.7937
S_h^0	0.5000
S_m^0	0.2500
μ_m	-12.3150

using a bar plot. Parameters with positive elasticity values increase R_0 when they rise, whereas negative values indicate that increasing the parameter reduces R_0. From Table 4.5

Copyright © 2025 ASSA.

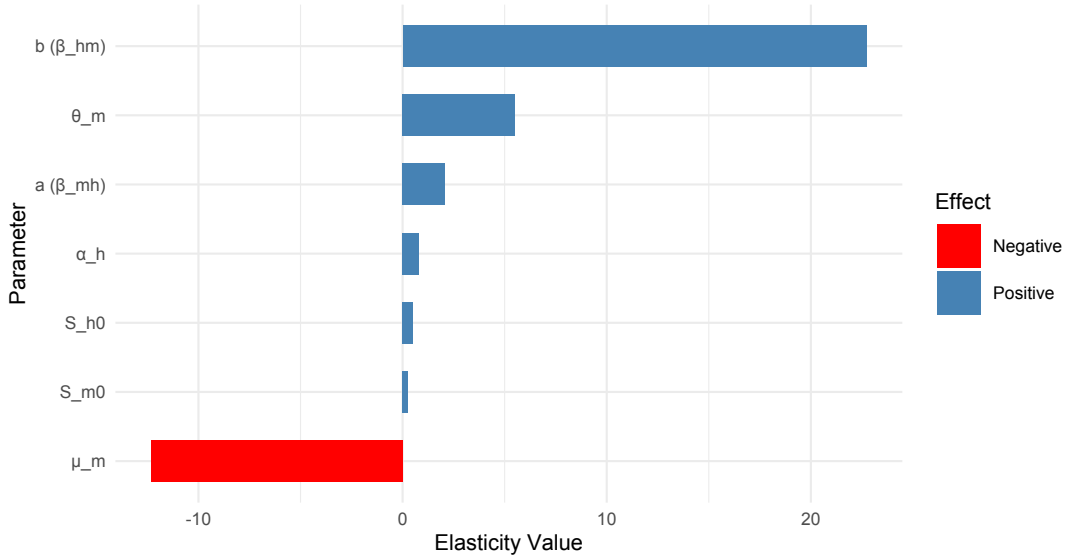

Fig. 4.6. Normalized indices of R_0 for key parameters.

and Fig. 4.6, the analysis reveals that the transmission probability from mosquito to human ($b = \beta_{hm}$) exerts the strongest positive influence on the basic reproduction number R_0 ($S_b = 22.73$), indicating that even small increases in mosquito infectivity can substantially amplify malaria transmission intensity. Similarly, the mosquito incubation rate ($\theta_m = 5.49$) and the human-to-mosquito transmission probability ($a = \beta_{mh}$) also contribute positively to R_0, emphasizing their roles in sustaining transmission. Conversely, the mosquito mortality rate ($\mu_m = -12.32$) exhibits a strong negative elasticity, implying that higher mosquito death rates significantly reduce the spread of infection. Other parameters, including the human exposure rate (α_h) and the initial susceptible populations (S_h^0, S_m^0), show moderate effects on R_0. The results suggest that control measures targeting reductions in mosquito survival and infectivity are the most effective strategies for driving R_0 below unity and curbing malaria transmission.

5. CONCLUSION

This study presents a temperature-dependent malaria transmission model that integrates mosquito aquatic-stage dynamics and heterogeneous extrinsic incubation periods to improve the representation of climate–disease interactions. Through incorporating short- and long-term EIP processes and modelling temperature-driven maturation delays, the framework provides a better understanding of how environmental variability influences mosquito population dynamics and transmission potential. The model captures essential nonlinear effects of temperature and rainfall on mosquito survival, biting rates, and developmental rates, thereby offering a more robust foundation for predicting malaria risk under changing climatic conditions. The analytical and numerical results highlight the significance of the extrinsic incubation period as a key driver of transmission intensity and highlight the sensitivity of mosquito maturation and infection processes to temperature fluctuations. These findings demonstrate that climate-based malaria models must accurately represent both vector ecology and parasite development to provide reliable forecasts. The proposed model contributes to ongoing efforts to develop climate-informed surveillance tools that support targeted, timely, and effective vector control interventions. Future research may extend this framework by

Copyright © 2025 ASSA.

incorporating stochastic climate variability, spatial heterogeneity, aquatic dynamics, and intervention strategies such as insecticide-treated nets and larval source management. Such extensions will further strengthen the capacity of mathematical models to guide public health planning and reduce the burden of malaria in endemic regions.

REFERENCES

1. Barreaux, A. M., Barreaux, P., Thievent, K. & Koella, J. C. (2016) Larval environment influences vector competence of the malaria mosquito Anopheles gambiae, *Malaria World J*, **7**(8), 1–6.
2. Blanford, J. I., Blanford, S., Crane, R. G., Mann, M. E., Paaijmans, K. P., et al. (2013) Implications of temperature variation for malaria parasite development across Africa, *Scientific reports*, **3**(1), 1–1.
3. Christiansen-Jucht, C., Parham, P. E., Saddler, A., Koella, J. C. & Basáñez, M. G. (2014) Temperature during larval development and adult maintenance influences the survival of Anopheles gambiae S.S, *Parasites & vectors*, **7**(1), 489.
4. Wang, X. & Zhao, X. Q. (2017) A periodic vector-bias malaria model with incubation period, *SIAM Journal on Applied Mathematics*, **77**(1), 181–201.
5. MacLeod, D. A. & Morse, A. P. (2014) Visualizing the uncertainty in the relationship between seasonal average climate and malaria risk, *Scientific reports*, **4**, 7264.
6. Chaves, L. F., Higa, Y., Lee, S. H., Jeong, J. Y., Heo, S. T., et al. (2013) Environmental forcing shapes regional house mosquito synchrony in a warming temperate island, *Environmental entomology*, **42**(4), 605–13.
7. Yoo, E. H., Chen, D., Diao, C. & Russell, C. (2016) The effects of weather and environmental factors on West Nile virus mosquito abundance in Greater Toronto area, *Earth Interactions*, **20**(3), 1–22.
8. Beck-Johnson, L. M., Nelson, W. A., Paaijmans, K. P., Read, A. F., Thomas, M. B., et al. (2017) The importance of temperature fluctuations in understanding mosquito population dynamics and malaria risk, *Royal Society open science*, **4**(3), 160969.
9. Beck-Johnson, L. M., Nelson, W. A., Paaijmans, K. P., Read, A. F., Thomas, M. B., et al. (2013) The effect of temperature on Anopheles mosquito population dynamics and the potential for malaria transmission, *PLOS one*, **8**(11), e79276.
10. Mordecai, E. A., Paaijmans, K. P., Johnson, L. R., Balzer, C., Ben-Horin, T., et al. (2013) Optimal temperature for malaria transmission is dramatically lower than previously predicted, *Ecology letters*, **16**(1), 22–30.
11. Ngarakana-Gwasira, E. T., Bhunu, C. P., Masocha, M. & Mashonjowa, E. (2016) Assessing the role of climate change in malaria transmission in Africa, *Malaria research and treatment*, **2016**, 7104291.
12. Okuneye, K. & Gumel, A. B. (2017) Analysis of a temperature-and rainfall-dependent model for malaria transmission dynamics, *Mathematical biosciences*, **287**, 72–92.
13. Agusto, F. B., Gumel, A. B. & Parham, P. E. (2015) Qualitative assessment of the role of temperature variations on malaria transmission dynamics, *Journal of Biological Systems*, **23**(04), 1550030.
14. Lou, Y. & Zhao, X. Q. (2010) A climate-based malaria transmission model with structured vector population, *SIAM Journal on Applied Mathematics*, **70**(6), 2023–2044.
15. Vaidya, A., Bravo-Salgado, A. D. & Mikler, A. R. (2014) Modeling climate-dependent population dynamics of mosquitoes to guide public health policies, *Proc. of the 5th ACM Conference on Bioinformatics, Computational Biology, and Health Informatics* (Newport Beach, CA), 380–389.
16. Wang, W. & Zhao, X. Q. (2008) Threshold dynamics for compartmental epidemic models in periodic environments, *Journal of Dynamics and Differential Equations*, **20**(3), 699–717.

Copyright © 2025 ASSA.

17. Ngwa, G. A., Niger, A. M. & Gumel, A. B. (2010) Mathematical assessment of the role of non-linear birth and maturation delay in the population dynamics of the malaria vector, *Applied Mathematics and Computation*, **217**(7), 3286–313.
18. Shan, C., Fan, G. & Zhu, H. (2019) Periodic Phenomena and Driving Mechanisms in Transmission of West Nile Virus with Maturation Time, *Journal of Dynamics and Differential Equations*, **11**, 1–24.
19. Zheng, C., Zhang, F. & Li, J. (2014) Stability Analysis of a Population Model with Maturation Delay and Ricker Birth Function, *In Abstract and Applied Analysis*, **2014**, 136707.
20. Nie, L. F. & Xue, Y. N. (2017) The roles of maturation delay and vaccination on the spread of Dengue virus and optimal control, *Advances in Difference Equations*, **2017**(1), 278.
21. Nah, K., Nakata, Y. & Röst, G. (2014) Malaria dynamics with long incubation period in hosts, *Computers & Mathematics with Applications*, **68**(9), 915–930.
22. Traoré, B., Sangaré, B. & Traoré, S. (2017) A mathematical model of malaria transmission with structured vector population and seasonality, *Journal of Applied Mathematics*, **2017**(4), 1–15.
23. Singh, B. & Daneshvar, C. (2013) Human infections and detection of Plasmodium knowlesi, *Clinical microbiology reviews*, **26**(2), 165–184.
24. Abdelrazec, A. & Gumel, A. B. (2017) Mathematical assessment of the role of temperature and rainfall on mosquito population dynamics, *Journal of mathematical biology*, **74**(6), 1351–1395.
25. Okuneye, K., Eikenberry, S. E. & Gumel, A. B. (2019) Weather-driven malaria transmission model with gonotrophic and sporogonic cycles, *Journal of biological dynamics*, **13**(sup1), 288–324.
26. Wan, H. & Zhu, H. (2014) A new model with delay for mosquito population dynamics, *Mathematical Biosciences & Engineering*, **11**(6), 1395.
27. Gopalsamy, K. (2013) *Stability and oscillations in delay differential equations of population dynamics*. Berlin, Germany: Springer Science & Business Media.
28. Parham, P. E., Pople, D., Christiansen-Jucht, C., Lindsay, S., Hinsley, W., et al. (2012) Modeling the role of environmental variables on the population dynamics of the malaria vector Anopheles gambiae sensu stricto, *Malaria Journal*, **11**(1), 271.
29. Lakshmikantham, V., Leela, S., (Eds.) (1969) *Differential and Integral Inequalities: Theory and Applications: Volume I: Ordinary Differential Equations*, Cambridge, MA, USA: Academic press.
30. Van den Driessche, P. & Watmough, J. (2002) Reproduction numbers and sub-threshold endemic equilibria for compartmental models of disease transmission, *Mathematical biosciences*, **180**(1-2), 29–48.
31. Briat, C. (2017) Sign properties of Metzler matrices with applications, *Linear Algebra and its Applications*, **515**, 53–86.
32. Zhu, Y., Wang, Q. A., Li, W. & Cai, X. (2017) Uncertainty and sensitivity analysis to complex systems, *International Journal of Modern Physics C*, **28**(08), 1750109.
33. Wu, J., Dhingra, R., Gambhir, M. & Remais, J. V. (2013) Sensitivity analysis of infectious disease models: methods, advances and their application, *Journal of The Royal Society Interface*, **10**(86), 20121018.
34. Helton, J. C. & Davis, F. J. (2003) Latin hypercube sampling and the propagation of uncertainty in analyses of complex systems, *Reliability Engineering & System Safety*, **81**(1), 23–69.
35. Marino, S., Hogue, I. B., Ray, C. J. & Kirschner, D. E. (2008) A methodology for performing global uncertainty and sensitivity analysis in systems biology, *Journal of theoretical biology*, **254**(1), 178–196.
36. Niger, A. M. & Gumel, A. B. (2008) Mathematical analysis of the role of repeated exposure on malaria transmission dynamics, *Differential Equations and Dynamical*

Copyright © 2025 ASSA.

Systems, **16**(3), 251–287.
37. Paaijmans, K. P., Read, A. F. & Thomas, M. B. (2009) Understanding the link between malaria risk and climate, *Proceedings of the National Academy of Sciences*, **106**(33), 13844–13849.
38. Chitnis, N., Cushing, J. M. & Hyman, J. M. (2006) Bifurcation analysis of a mathematical model for malaria transmission, *SIAM Journal on Applied Mathematics*, **67**(1), 24–45.
39. Tesla, B., Demakovsky, L. R., Mordecai, E. A., Bonds, M. H., Ngonghala, C. N., et al. (2018) Impacts of temperature on Zika virus transmission potential: combining empirical and mechanistic modeling approaches, *bioRxiv*: 259531, [Online]. Available: https://www.biorxiv.org/content/10.1101/259531v2
40. World Health Organization (2024) *Global malaria programme operational strategy 2024-2030*, [Online]. Available: https://www.who.int/publications/i/item/9789240090149
41. Alemu, A., Lemma, B., Bekele, T., Geshere, G., Simma, E. A., et al. (2024) Malaria burden and associated risk factors among malaria suspected patients attending health facilities in Kaffa zone, Southwest Ethiopia, *Malaria Journal*, **23**(1), 397.
42. Takken, W., Charlwood, D., & Lindsay, S. W. (2024). The behaviour of adult Anopheles gambiae, sub-Saharan Africa's principal malaria vector, and its relevance to malaria control: a review. *Malaria journal*, **23**(1), 161.
43. Belay, A. K., Asale, A., Sole, C. L., Kinya, F., Yusuf, A. A., et al. (2024) Vectorial drivers of malaria transmission in Jabi Tehnan district, Amhara regional State, Ethiopia, *Scientific Reports*, **14**(1), 13669.
44. Modu, B., Polovina, N., & Konur, S. (2023) Agent-based modeling of malaria transmission, *IEEE Access*, **11**, 19794–19808.
45. Abioye, A. I., Peter, O. J., Oguntolu, F. A., Ayoola, T. A., & Oladapo, A. O. (2023). Global stability and sensitivity analysis of basic reproduction number of a malaria model, *Advances in Systems Science and Applications*, **23**(4), 90–103.

Copyright © 2025 ASSA.